

Simulation of chloride ion profile into repaired crack concrete

Md. Shafiqul Islam and Md. Mahmud Sazzad

*Department of Civil Engineering
Rajshahi University of Engineering and Technology, Kazla 6204, Rajshahi, Bangladesh*

Received 10 September 2007

Abstract

Chloride induced corrosion of steel in concrete is a threatening problem in coastal and marine environment. The durability of structures decreases and hampers efficient structural performance. In reality, cracks are often generated at cover concrete. In that case, the transportation of chloride ion (Cl^-) may take only a few hours to reach the steel, while transportation through uncracked concrete would take a longer time. Moreover, if some part of concrete is repaired by polymer modified cementitious mortar, the transportation of Cl^- ion is affected by the combination of two different materials. In this study, experiments were done with partially repaired crack concrete to simulate real field structure. A model is proposed to calculate the concentration profile inside a partially repaired crack concrete with the help of a 2-dimensional FORTRAN program.

© 2008 Institution of Engineers, Bangladesh. All rights reserved.

Keywords: Chloride, diffusion, transport properties, cracking

1. Introduction

Chloride induced corrosion of steel in concrete structures, affected by deicing salt, coastal and a marine environment is a great problem everywhere in the world. A considerable number of structures cease to function adequately. Extensive research was conducted over the past decades to study the transport properties of concrete. The disadvantage is that all predictions are carried out considering a 'perfect' and uncracked concrete. The fact that most reinforced concrete structures having cracks are often ignored (Pettersson and Sandberg 1997). Once these cracks take place, the transport properties of material change drastically and it is no longer reasonable to assume that durability life-span based on uncracked properties will hold. A debate among the researchers on crack width and corrosion rate relationships has been continuing for a long time. Several researches found little relationships between crack width and corrosion rate (Schweitzer 1986).

Moreover, in case of partially repaired concrete, the majority of cracks resulted from drying shrinkage within the repair material and thus crack is generated at the interface between concrete and repair material which helps the penetration of aggressive material faster than usual. This paper reports the experimental investigation on Cl⁻ ion penetration in repaired crack concrete and proposed a simulation model based on the empirical equations.

2. Research significance

If a part of concrete is repaired, the majority of cracks resulted from drying shrinkage within the repair part. These cracks act as doors to H₂O, O₂, CO₂, Cl⁻ to go through. Most of the previous researches dealt with the placement of repair material at the top of concrete substrate. In this study it is the first time that touches most critical zone, where repair material is placed by the side of concrete and crack occurs at the interface of two materials. In this context, the study is significant in cases of repaired concrete having crack and thus to enrich the concrete technology.

3. Experimental program

3.1 Mix proportion

Table 1 lists the mix proportions of concrete employed as test specimens. In this study repair material used was Emaco S98P. It is a ready to use polymer modified cementitious mortar. The mixing proportion of Emaco S98P is shown in Table 2.

Table 1
Mix proportions of concrete

W/C	G _{max} in. (mm)	lb/ft ³ (kg/m ³) (s/a=45.5)				
		W	C	S	G	AE
0.55	0.79 (20)	10.99 (176)	20.04 (321)	50.19 (804)	61.74 (989)	0.13 (2.083)

Table 2
Mix proportions of Emaco

Emaco S98P lb (kg)	Water lb (kg)
55.125 (25)	8.82 (4)

3.2 Specimen geometry

The specimen had a square cross section (Figures 1-2) of 3.94 in. [100 mm] (W) x 3.94 in. [100 mm] (H) x 14.80 in. [376 mm] (L). One deformed steel bar of 0.394 in. [10 mm] in diameter was embedded longitudinally with cover depth of 0.79 in. [20 mm].

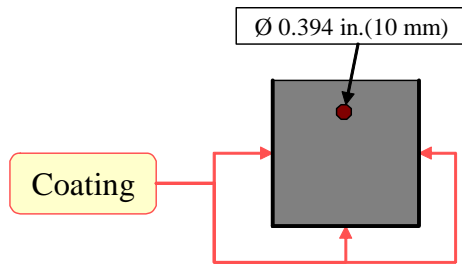


Fig. 1. Cross section of specimen.

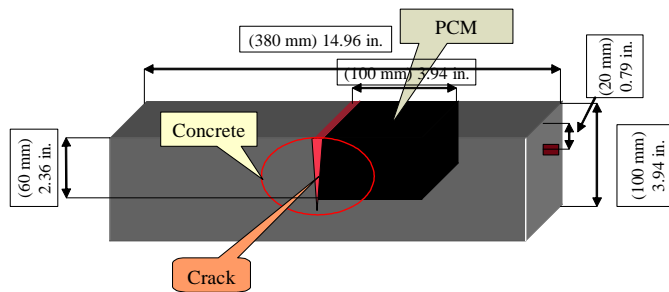
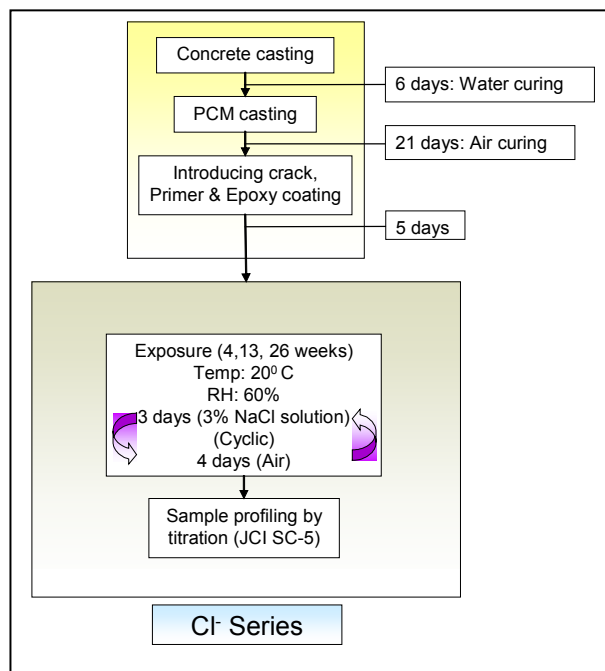


Fig. 2. Side view of specimen.

3.3 Curing and exposure condition



3.4 Cracking

The specimens were subjected to 3-point loading to generate a flexural crack at centre (the interface between concrete and PCM) as shown in Fig. 3. Crack widths were measured at three points on crack by (PI-5-50) displacement transducer (Fig. 4) and the average of three values was taken.

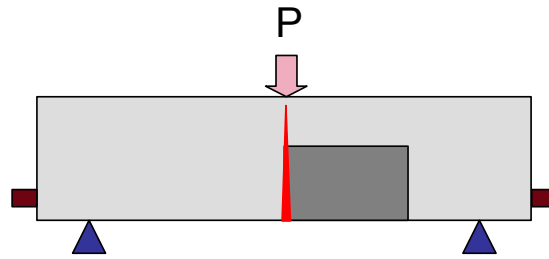


Fig. 3. 3-point loading.

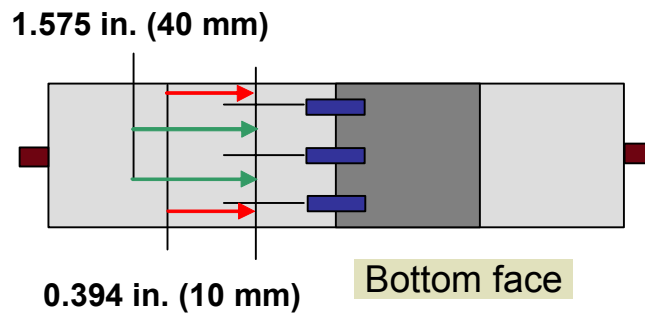


Fig. 4. PI gaugs location.

3.5 Specimen designation

Table 3 shows the introduction of all the test specimens. The specimens were exposed to cyclically 3% NaCl solution for 3 days and in air for 4 days under controlled temperature 20°C and RH 60%.

Total 21 specimens were cast for chloride series. Crack depth ranges from 1.18 in. [30 mm] to 3.54 in. [90 mm].

Cl: specimens were subjected to cyclically wet-dry condition, RB: specimens simulate a repaired beam consisting of old concrete and newly placed PCM, C: specimens were cast only by concrete, P: specimens were cast only using PCM, C0.025: represents the width of crack in mm.

3.6 Total chloride content

Total chloride contents were measured according to standard test method of JCI SC5 (1987). The samples were taken as shown in Fig. 5.

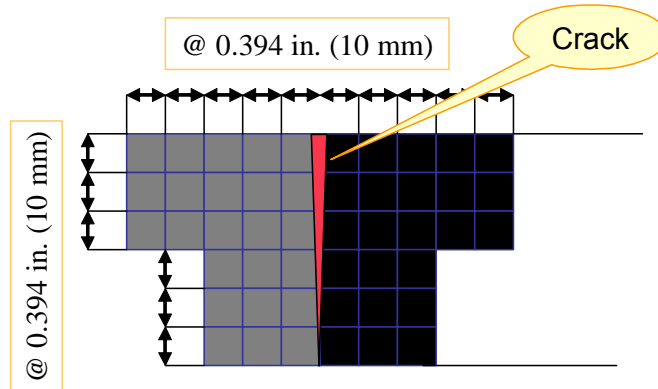


Fig. 5. Chloride profile

Table 3
Specimen introduction

Designation	1 st part		Middle part			Last part	Exposure duration (week)
	CI	RB	C	P	C		
	Cyclic wet-dry	Concrete +PCM	Concrete	PCM	Crack width in. (mm)		
CI RB C0.025	⊙	⊙			9.84xE-04 (0.025)	4, 13, 26	
CI RB C0.05	⊙	⊙			1.97xE-03 (0.05)	4, 13, 26	
CI RB C0.075	⊙	⊙			2.95xE-03 (0.075)	4, 13, 26	
CI RB C0.2	⊙	⊙			7.87xE-03 (0.2)	4, 13, 26	
CI RB C1.0	⊙	⊙			0.039 (1.0)	4, 13, 26	
CI C C0.0	⊙		⊙		No crack	4, 13	
CI P C0.0	⊙			⊙	No crack	4, 13	
CI RB C0.0	⊙	⊙			No crack	4, 13	

4. Chloride ion profile by interpreting the experimental results

4.1 Aim of study

Figures 6 and 7 show the Cl⁻ ion distribution inside concrete (right side) and PCM (left side). Although there is no crack, a big difference in the concentration is found. Therefore the experiment is aimed to consider the combination of material.

Figures 8 and 9 show the Cl⁻ ion distribution in concrete and PCM having crack at the interface. It is clearly observed that Cl⁻ ion accumulates near the crack. That is why the study is aimed to quantify the effect of crack width on Cl⁻ distribution.

4.2 Surface Cl⁻ (C_o) for sound part and apparent diffusion coefficient (D) from the best-fit-curves

Sound part represents the portion where the concentration values are not influenced by the existence of cracks. Surface Cl⁻ (C_o) for sound part and apparent diffusion coefficient (D) are obtained from the best-fit-curves from experimental data using Crack's error function equation as written below.

$$C(x, t) = C_o \operatorname{erf} \left(1 - \frac{x}{2\sqrt{Dt}} \right) \quad (1)$$

where, C(x, t): concentration of chloride at any distance from exposed surface at any time; C_o: surface chloride for sound part; x: distance from exposed surface; D: apparent diffusion coefficient; t: time.

Table 4
Summary of Surface Cl⁻ (C_o) for sound part
and apparent diffusion coefficient (D)

Time (day)	Specimen ID	Concrete			PCM		
		C _o	D	S	C _o	D	S
28	CIRBC0.025D28	0.6	3.87 (2.5)	0.0037	0.4	2.33 (1.5)	0.0001
	CIRBC0.05D28	0.58	3.87 (2.5)	0.0038	0.4	2.33 (1.5)	0.000001
	CIRBC0.075D28	0.5	3.87 (2.5)	0.0005	0.4	3.10 (2.0)	0.0016
	CIRBC0.2D28	0.52	3.87 (2.5)	0.0001	0.42	3.10 (2.0)	0.0022
	CIRBC1.0D28	0.55	3.25 (2.1)	0.0049	0.42	3.10 (2.0)	0.000081
91	CIRBC0.025D91	0.95	2.63 (1.7)	0.0072	0.7	1.55 (1.0)	0.0052
	CIRBC0.05D91	1.05	2.02 (1.3)	0.028	0.65	1.71 (1.1)	0.0078
	CIRBC0.075D91	1.0	3.10 (2.0)	0.0085	0.64	2.02 (1.3)	0.0101
	CIRBC0.2D91	1.0	3.10 (2.0)	0.0021	0.72	2.02 (1.3)	0.0429
	CIRBC1.0D91	0.95	2.79 (1.8)	0.0117	0.7	2.17 (1.4)	0.0038
182	CIRBC0.025D182	1.35	2.17 (1.4)	0.0251	0.9	1.86 (1.2)	0.0242
	CIRBC0.05D182	1.55	2.02 (1.3)	0.0409	0.8	1.71 (1.1)	0.0179
	CIRBC0.075D182	1.3	2.17 (1.4)	0.0928	0.8	1.71 (1.1)	0.001
	CIRBC0.2D182	1.25	1.55 (1.0)	0.0098	0.9	1.09 (0.7)	0.0216
	CIRBC1.0D182	1.45	2.17 (1.4)	0.0104	0.88	2.33 (1.5)	0.0034

C_o = % weight of sample, D = E-08 in²/sec, (D = E-05 mm²/sec)

The best fit was indicated by minimizing the sum "S" given by the following equation.

$$S = \sum_{n=1}^N \Delta C^2(n) = \sum_{n=1}^N [C_m(n) - C_c(n)]^2 \quad (2)$$

N: the number of concrete layers sampled; C_m(n): measured chloride content; C_c(n): Calculated chloride content.

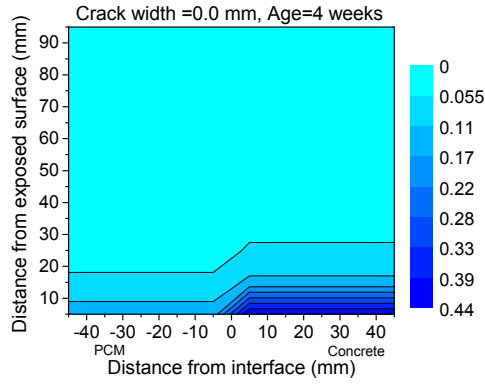


Fig. 6. Chloride profile for no cracked specimen (SI).

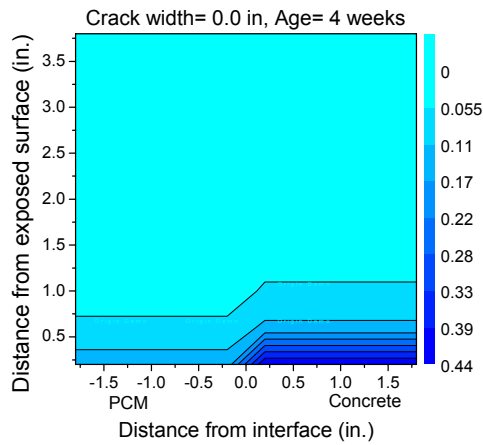


Fig. 7. Chloride profile for no cracked specimen (in.).

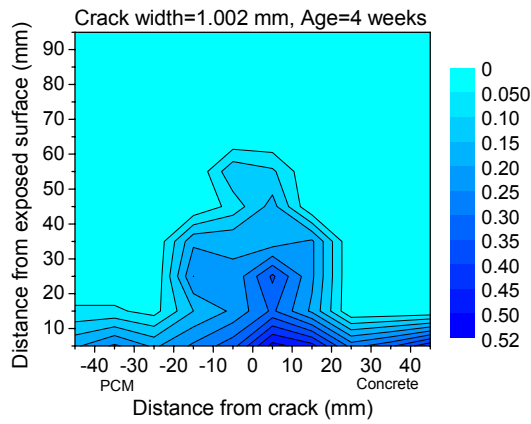


Fig. 8. Chloride profile for cracked specimen (SI).

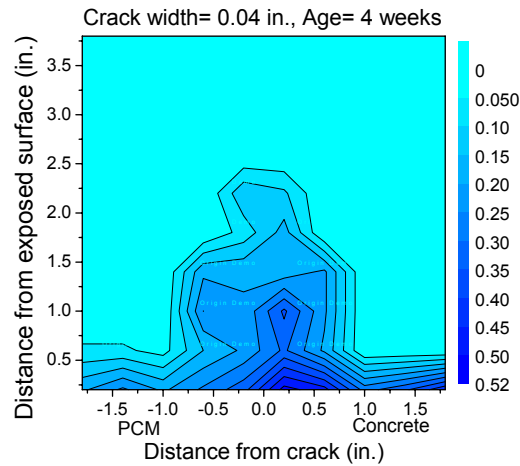


Fig. 9. Chloride profile for cracked specimen (in.).

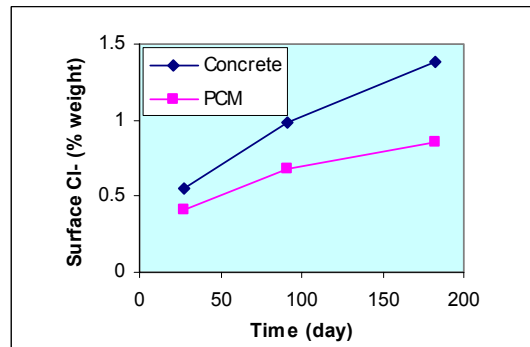


Fig. 10. Surface chloride for sound part.

Form the Table 4 it is found that that surface chloride (C_o) does not change rapidly with the change of crack width. But as the time increases surface chloride (C_o) increases for both concrete and PCM as shown in Fig. 10.

Therefore a new function $f(t)$ is included in Dr. Pa Pa Win's model to calculate surface chloride (C_o). Diffusion coefficient (D) is taken as the average value found for different crack widths and different time series.

4.3 Modified Pa Pa Win's model

$$C_o = 3.9(d)^{0.56} xf(t) \quad (3)$$

$$d = \frac{\text{[Time parameter]} \times 0.61 \times V_p \times C_{salt} \times P_{solution}}{C_e} \quad (4)$$

$$P_{solution} = \frac{P_{water} + 1000 \times C_{salt}}{1 + \frac{C_{salt}}{P_{salt}}} \tag{5}$$

0.61 is the % molar mass of Cl⁻ ions in NaCl; V_p: open pore volume in (%).

$$V_p (\%) = 21.4 \left(\frac{W}{C} \right)^{0.54} \tag{6}$$

P_{solution}: density of salt solution (kg/m³); C_{salt}: concentration of salt; C_e: cement content (kg/m³); P_{water} is taken as 998.2 kg/m³ at 20⁰C; P_{salt}: specific gravity of NaCl which is 2.165.

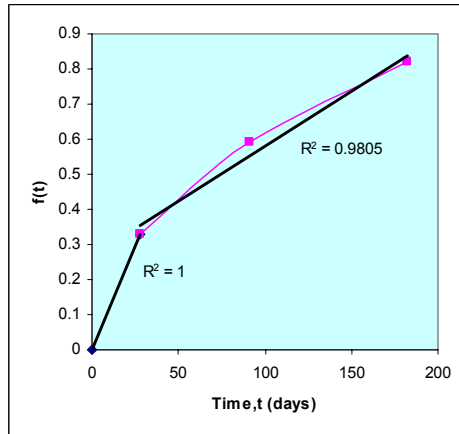


Fig. 11. Time parameter f(t) for concrete.

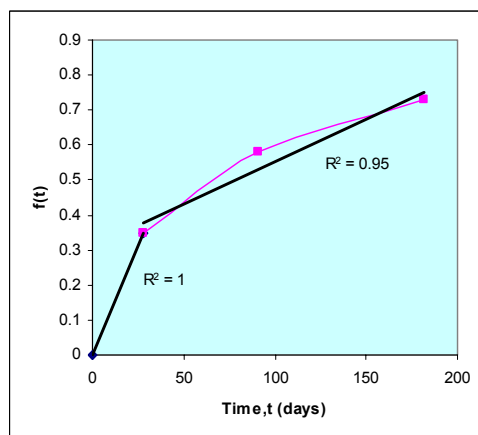


Fig. 12. Time parameter f(t) for PCM.

For concrete:

$$f(t) = 0.118(t) \quad 0 \leq t \leq 28 \quad (7)$$

$$f(t) = 0.0031(t) + 0.2654 \quad 28 \leq t \leq 182 \quad (8)$$

For PCM:

$$f(t) = 0.0125(t) \quad 0 \leq t \leq 28 \quad (9)$$

$$f(t) = 0.0024(t) + 0.3116 \quad 28 \leq t \leq 182 \quad (10)$$

4.4 Effect of material combination on surface chloride

The Figure 13 shows the pattern of material combination. The surface chloride (C_{ocr}) for crack zone is different from that of sound part (C_o).

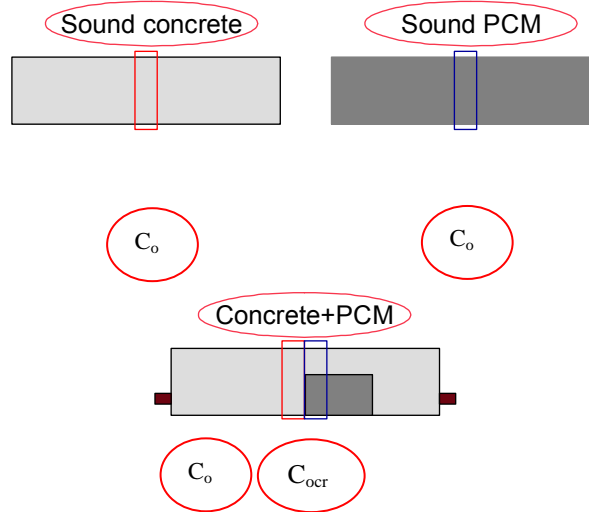


Fig. 13. Schematic view of material combination

From Fig. 14 and Fig. 15 it is clear that the surface chloride concentration at the crack zone in concrete is higher when concrete is cast combined with PCM rather than when it is cast as a single material.

On the other hand, the surface chloride concentration at the crack zone in PCM is lower (Fig. 16 and Fig. 17) when PCM is cast combined with concrete rather than when it is cast as a single material.

Surface chloride concentration at crack zone is calculated using the equation 1 and is plotted in the above figures with respect to time.

For concrete:

$$C_{ocr} = 0.0232(t) \quad 0 \leq t \leq 28 \quad (11)$$

$$C_{ocr} = 0.0055(t) + 0.5211 \quad 28 \leq t \leq 182 \quad (12)$$

For PCM :

$$C_{opcr} = 0.0121(t) \quad 0 \leq t \leq 28 \tag{13}$$

$$C_{opcr} = 0.0035(t) + 0.2709 \quad 28 \leq t \leq 182 \tag{14}$$

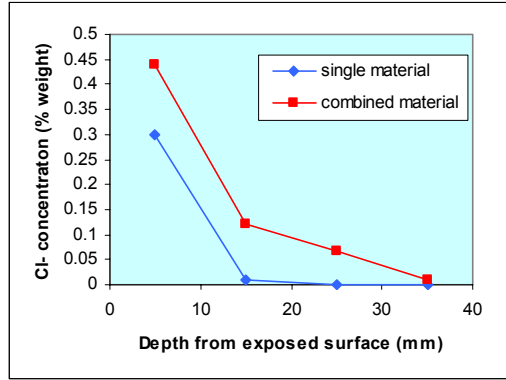


Fig. 14. Cl⁻ concentration in concrete as single and combined material (SI).

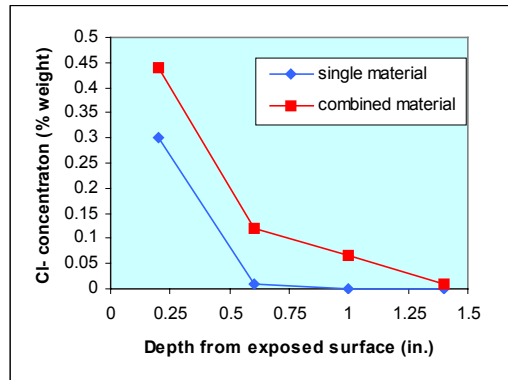


Fig. 15. Cl⁻ concentration in concrete as single and combined material (in.).

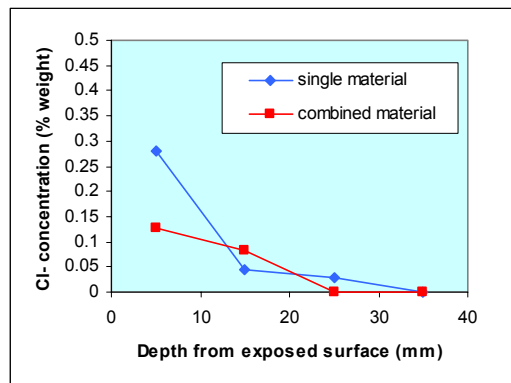


Fig. 16. Cl⁻ concentration in PCM as single and combined material (SI)

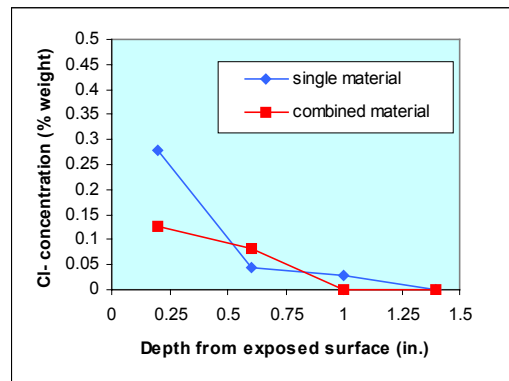


Fig. 17. Cl⁻ concentration in PCM as single and combined material (in.)

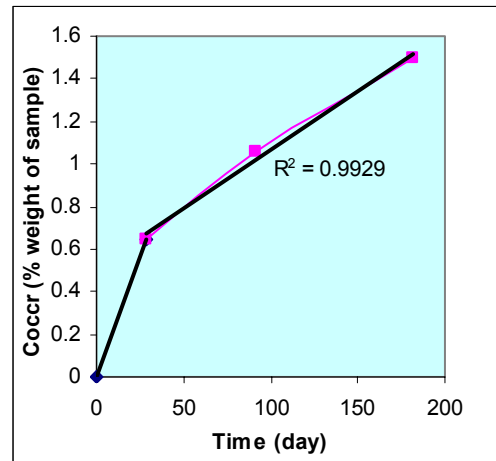


Fig. 18. Surface chloride at crack zone for concrete

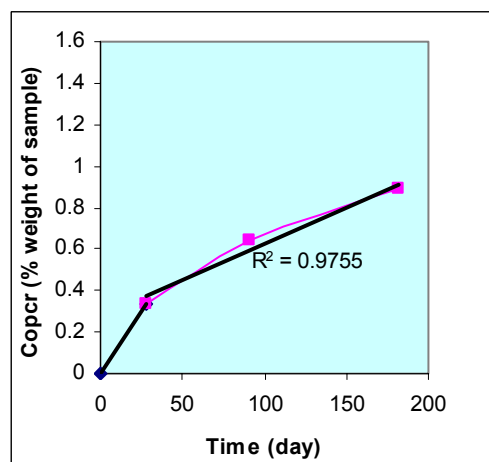


Fig. 19. Surface chloride at crack zone for PCM.

4.5 Chloride ion content along crack

Fig. 20 shows the image of chloride ion content at crack zone which can be found using the model below.

$$C_{cr}(x) = \alpha\sqrt{x} + C_{ocr} \tag{15}$$

C_{cr} : chloride ion content along crack in % weight of sample; C_{ocr} : the surface chloride at crack zone in % weight of sample; x : distance from exposed surface in cm.; α : a parameter named as reduction factor that depends on crack width (mm) and exposure duration (day).

The relationship between reduction factor (α) and crack width (W_{cr}) is shown in Fig. 21, Fig. 22, Fig. 23 and Fig. 24. The constants c_a , c_b for concrete and p_a , p_b for PCM are related with 4, 13 and 26 weeks exposure durations for the convenience of calculation.

It is found that the reduction factor increases with the increase of crack width. When the crack width gets larger, the evaporation will also increase during drying which helps increasing the Cl^- concentration. The relationship between reduction factor and crack width well agrees with the above assumption.

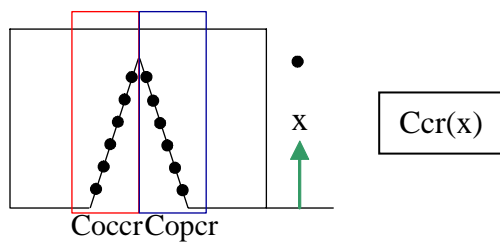


Fig. 20. Schematic view along crack

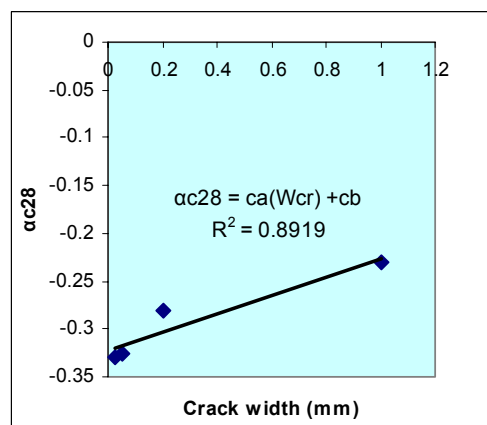


Fig. 21. Reduction factor for concrete Exposure age: 4 weeks (SI).

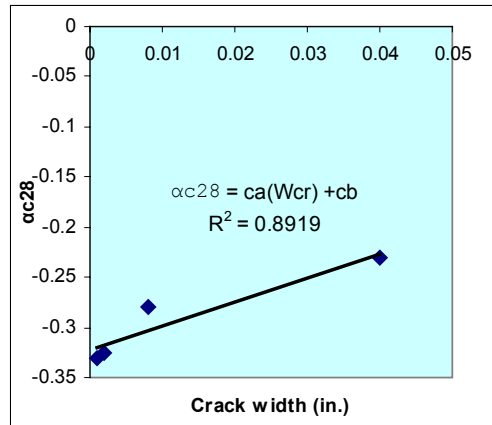


Fig. 22. Reduction factor for concrete Exposure age: 4 weeks (in.).

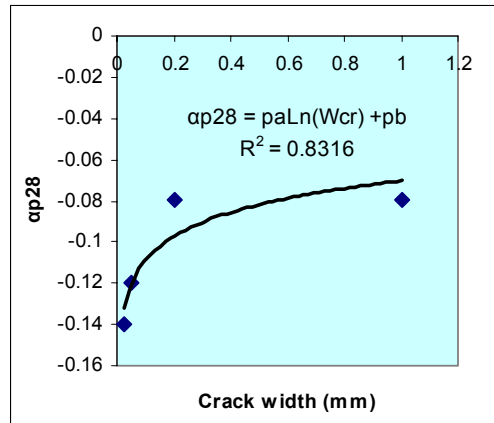


Fig. 23. Reduction factor for PCM Exposure age: 4 weeks (SI).

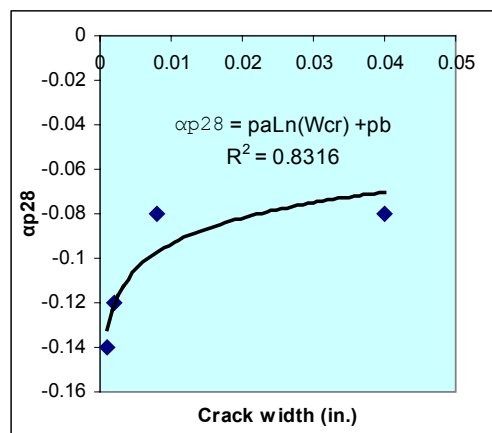


Fig. 24. Reduction factor for PCM Exposure age: 4 weeks (in.).

5. Model of chloride ion transport in repaired crack concrete

5.1 Assumption

The authors assume some steps to calculate the concentration of chloride ion inside cracked concrete with repair patch.

Steps

1. Calculation of C_0 (surface Cl^- for sound part) & D (Diffusion coefficient).
2. Calculation of Cl^- concentration along crack one dimensionally.

Parameters:

- α = function of W_{cr} & t ;
- C_{ocr} = Boundary Cl^- for cracked part;

Fixing this crack Cl^- as one boundary for whole concrete.

3. Calculation of Cl^- profile for whole concrete two dimensionally.

The experimental specimen is drawn at the top of Fig. 25 and locations for assumption are drawn below to make easily understandable.

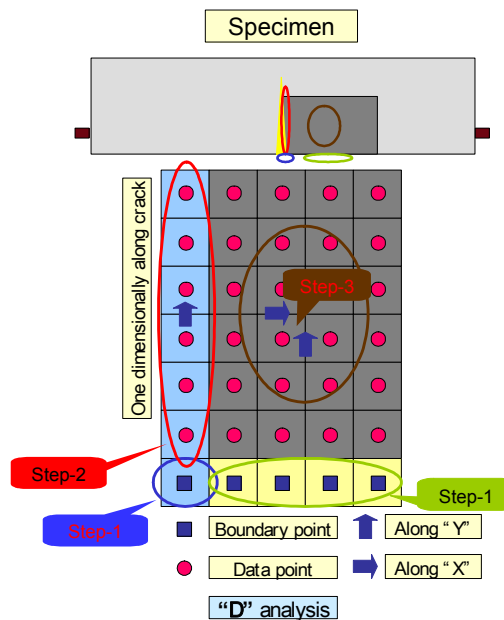


Fig. 25. Schematic diagram of the assumption

The surface chloride for sound part (C_o), apparent diffusion co-efficient (D) and surface chloride for cracked part (C_{ocr}) can be found using the equations as explained in the previous sections. Putting the values of crack width (W_{cr}) and exposure duration (t) and using the value of the surface chloride for cracked part (C_{ocr}), authors calculate the chloride ion content along crack one dimensionally. This chloride at crack is set as one boundary for the whole cracked concrete. Now we are able to know the distribution of chloride ion inside the whole cracked concrete utilizing the Fick's 2nd law of diffusion considering two dimensional penetrations with the help of finite difference method.

5.2 Analysis method

Fick's 2nd law is used in non-steady diffusion, i.e. when concentration within the diffusion volume changes with respect to time.

$$\frac{\partial C}{\partial t} = D \left(\frac{\partial^2 C}{\partial x^2} + \frac{\partial^2 C}{\partial y^2} \right) \quad (16)$$

Equation 16 is the two dimensional form of Fick's law to analyze the diffusion mechanism. Considering three points on the x-axis separated by dx, and with the help of Taylor's expansion, function C(x,y) can be written as follows,

$$\frac{\partial^2 C}{\partial x^2} = \frac{C_{i-1} - 2C_i + C_{i+1}}{dx^2} \quad (17)$$

Similarly, taking three points along y-axis,

$$\frac{\partial^2 C}{\partial y^2} = \frac{C_{j-1} - 2C_j + C_{j+1}}{dy^2} \quad (18)$$

By superimposing 17 and 18, we arrive at 5-point stencil and 'C' requires two subscripts, one for 'i' or x-direction and the other for 'j' or y-direction.

$$\frac{\partial^2 C}{\partial x^2} + \frac{\partial^2 C}{\partial y^2} = \frac{C_{i-1} - 2C_i + C_{i+1}}{dx^2} + \frac{C_{j-1} - 2C_j + C_{j+1}}{dy^2} \quad (19)$$

$$\frac{\partial C}{\partial t} = \frac{C_{t+dt} - C_t}{dt} \quad (20)$$

Assuming $dx=dy$, finally by rearranging we get,

$$C_{t+dt} = C_t + D \times \frac{dt}{dx^2} [\{ C_{j,i-1} - 2C_{j,i} + C_{j,i+1} \} + \{ C_{j-1,i} - 2C_{j,i} + C_{j+1,i} \}] \quad (21)$$

Considering the assumption and proposed equations shown in previous sections and with the help of above finite differentiation scheme, the concentration profile in a partially repaired crack concrete can be calculated.

6. Verification of proposed scheme

The chloride ion profile in the cracked zone in concrete and PCM at the age of 182 days are shown in Fig. 26, Fig. 27, Fig. 28 and Fig. 29 respectively. These show well matching between experimental and calculation results.

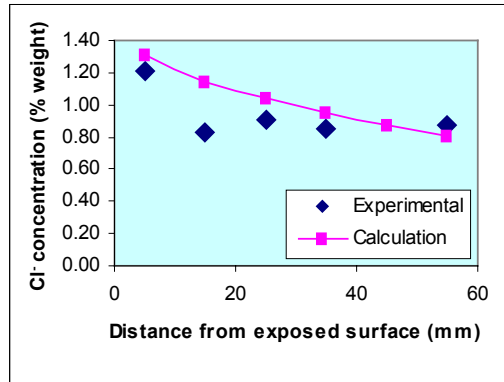


Fig. 26. Cl⁻ content along crack in concrete (SI)

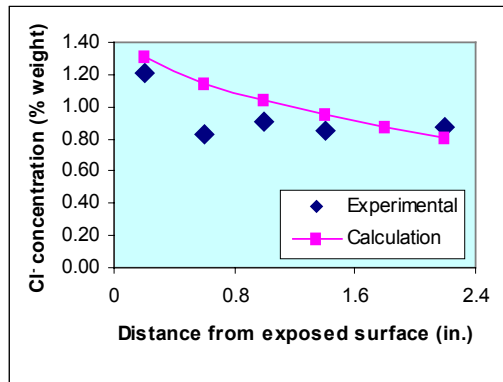


Fig. 27. Cl⁻ content along crack in concrete (in.)

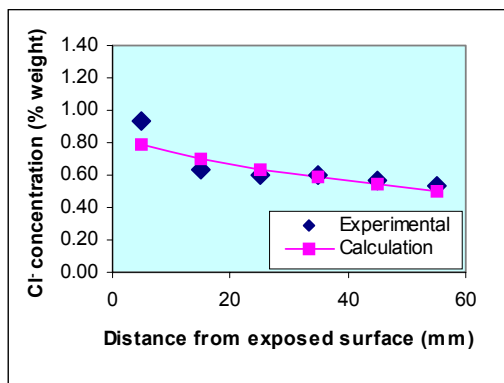


Fig. 28. Cl⁻ content along crack in PCM (SI)

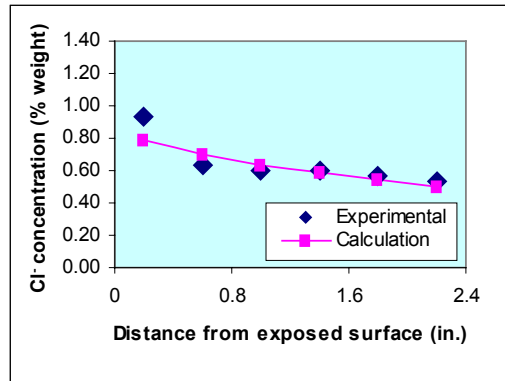


Fig. 29-Cl⁻ content along crack in PCM (in.).

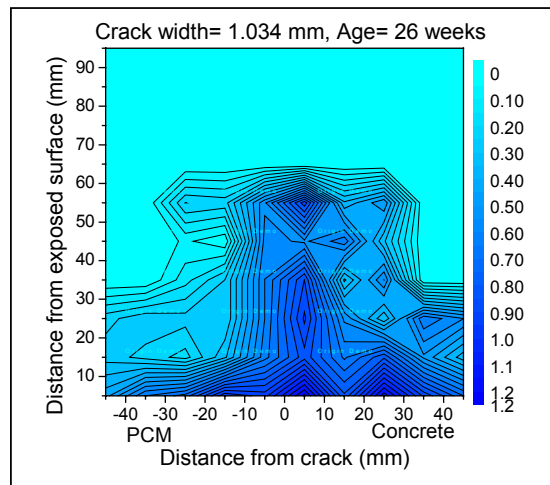


Fig. 30. Cl⁻ profile for whole partially repaired crack concrete (Experiment) [SI]

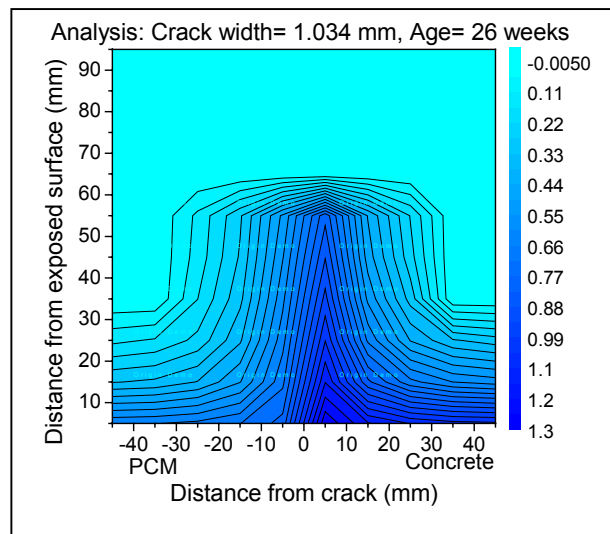


Fig. 31. Cl⁻ profile for whole partially repaired crack concrete (Experiment) [in.]

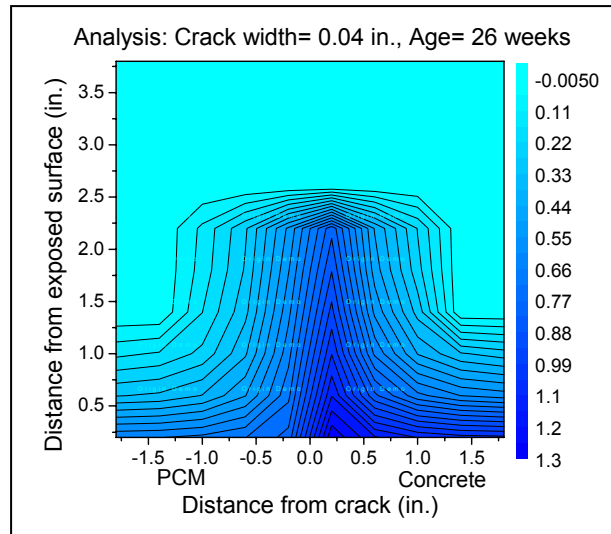


Fig. 32. Cl^- profile for whole partially repaired crack concrete (Analysis) [in.]

Figures 30-32 show the chloride ion profile in the whole partially repaired crack concrete. Fig. 30 and Fig. 31 is obtained from experimental data of the specimen with 0.0407 in. [1.034 mm] crack at the age of 182 days and Fig. 32 and Fig. 33 are obtained from analysis data of the specimen with 0.0407 in. [1.034 mm] crack at the age of 182 days. They were well simulated by the proposed model. This result supports that proposed model possibly to evaluate chloride ion profile inside partially repaired crack concrete under cyclic wet-dry condition.

7. Conclusions

1. Surface chloride (C_o) for sound part remains unchanged with the change of crack width. But as the time increases surface chloride (C_o) increases for both concrete and PCM.
2. A newly introduced time parameter $f(t)$ is included in Dr. Pa Pa Win's model to calculate surface chloride (C_o) that also increases as exposure time increase.
3. Surface chloride concentration at the crack zone (C_{ocr}) in concrete is higher when concrete is cast in combination with PCM rather than when it is cast as a single material.
4. Surface chloride concentration at the crack zone (C_{ocr}) in PCM is lower when PCM is cast in combination with concrete rather than when it is cast as a single material.
5. Reduction factor ' α ' increases with the increase of crack width, but the rate of increase becomes flatter for larger crack width in case of PCM as compared to concrete.

Acknowledgements

One of authors would like to express his gratitude to Prof. Taketo Uomoto, The University of Tokyo, for giving support as his supervisor. Assoc. Prof. Toshiharu Kishi and Assoc. Prof. Yoshitaka Kato provided their valuable suggestions regarding this paper. The authors want to be deeply thankful to Mr. Tsugio Nishimura, Technician of Uomoto laboratory, for his continuous help during experiments.

Notations

erf	=	error function
C_o	=	surface chloride for sound part (% weight of sample)
$f(t)$	=	function of time
C_{ocr}	=	surface chloride for crack zone (% weight of sample)
C_{occr}	=	surface chloride for crack zone (% weight of sample) for concrete
C_{opcr}	=	surface chloride for crack zone (% weight of sample) for PCM
PCM	=	polymer modified cementitious mortar
ca, cb	=	constants used for concrete part
pa, pb	=	constants used for PCM part
α_c	=	reduction factor used for concrete
α_p	=	reduction factor used for PCM

References

- Hussein, N., Yada, K., Tanak, K., Sato, R., (2004), "Salty water penetration in concrete through cracks," International Seminar on Durability and Lifecycle Evaluation of Concrete Structures, 2004.
- JCI SC5 (1987), Standard Method of Examination Regarding the Corrosion and Corrosion Protection of Concrete Structure.
- Kato, E., Kato, Y., Uomoto, T., (2005), "Development of simulation model of chloride ion transportation in cracked concrete," Journal of Advanced Concrete Technology, 3, 85-94.
- Mangat, P. S., Limbachiya, M. C., (1999), "Effect of initial curing on chloride diffusion in concrete repair materials," Cement and Concrete Research, 29, 1475-1485.
- Mitra, A. K., "Finite Difference Method for the Solution of Laplace Equation," Department of Aerospace Engineering, Iowa State University.
- Mohammed, T. U., Otsuki, N., Hamada, H., (2001). "Oxygen permeability in cracked concrete reinforced with plain and deformed bars," Cement and Concrete Research, 31, 829-834.
- Mohammed, T. U., Otsuki, N., Hisada, M., Shibata, T., (2001), "Effect of crack width and bar types on corrosion of steel in concrete, Journal of Materials in Civil Engineering, 13, 194-201.
- Pettersson, K., Sandberg, P., (1997), "Chloride threshold levels, corrosion rates and service life for cracked high performance concrete," Durability of concrete, Fourth international conference, Sydney, Australia; CANMET/ ACI SP-170, Michigan, 1997, pp. 451-472.
- Schutter, G. D., (2000), "Durability of marine concrete structures damaged by early age thermal cracking," International RILEM Workshop of Life prediction and aging management of concrete structures, Cannes, France, Oct. 16-17, 2000.
- Schweitzer, P. A., (1986), "Corrosion and corrosion protection handbook".
- Win, P. P., Watanabe, M., Machida, A., (2004), "Penetration profile of chloride ion in cracked reinforced concrete," Cement and Concrete Research, 34, 1073-1079.